



28 which dissolve inorganic salts from the rock to obtain nutrients. This process "erodes" the rock, damaging its
29 surface structure and gradually weathering it. Given the prolific growth of aerophytic organisms on marble
30 surfaces, finding ways to prevent or reduce their growth is crucial for slowing down the weathering process of
31 stone cultural relics in the Temple of Heaven Park.

32

33 **Keywords:** Temple of Heaven Park, Beijing, China; marble; aerophytic algae; cyanobacteria; bioweathering.

34

35 **1. introduction**

36 The Temple of Heaven Park in Beijing, China, completed in the 18th year of the Yongle reign of the
37 Ming Dynasty (1420), has a history of 604 years to date. It is the largest existing ancient sacrificial building
38 complex in the world, where emperors of the Ming and Qing dynasties performed ceremonies to worship
39 heaven and pray for good harvests. In 1961, the State Council of China declared the Temple of Heaven a
40 "National Key Cultural Relic Protection Unit." In 1998, it was recognized as a "World Cultural Heritage"
41 site by UNESCO. The Hall of Prayer for Good Harvests is the core structure of the Temple of Heaven Park
42 and was the venue for the Qing Dynasty's grain prayer ceremonies. It consists of an upper building and a
43 lower terrace. The building is the Hall of Prayer for Good Harvests, while the terrace is a three-tiered
44 circular platform. Each level of the circular platform is surrounded by white marble railings with bluish-
45 white stone foundations. The upper level's corner columns are decorated with coiled dragons and water
46 spouts with chi-dragon heads. The middle level's corner columns feature flying phoenixes with phoenix-
47 head water spouts. The lower level's corner columns are adorned with cloud motifs and cloud-shaped water
48 spouts. Most of these white marble and bluish-white stones originate from the marble quarries in Dashiwo
49 Town, Fangshan District, Beijing (Wu and Liu, 1996; Lü and Wei, 2020). Among the various stone materials
50 used for cultural relics, such as granite, marble, sandstone, limestone, and conglomerate, marble is the
51 softest and most easily weathered. The white marble, in particular, is even softer and more prone to
52 weathering (Ye and Zhang, 2019). However, white marble is pure white, solid yet fine-grained, and easy to
53 carve. It is often used for intricate carvings such as palace railings, imperial steps, and various stone tablets,
54 making it a highly prized building material. Bluish-white stone is generally chosen for load-bearing
55 components like pedestal stones, cap stones, stone bridges, and slabs. White marble and bluish-white stone
56 became the most favored stone materials for royal constructions, but they are also the most susceptible to



57 weathering among stone cultural relics.

58 Marble, when exposed to natural environments over long periods, not only endures physical and
59 chemical weathering but also undergoes biological weathering. Biological weathering refers to the
60 degradation caused by biological activities, which impacts the rock through growth and activity of
61 organisms. This process not only alters the physical and chemical properties of the marble surface but also
62 leads to the formation of unique biological communities, primarily aerophytic cyanobacteria. Chinese
63 scholars have conducted numerous studies on the physical and chemical weathering of marble (Liu et al.,
64 2005, 2006; Liu, 2007; Wang, 2010; Zhang et al., 2013; Zhang et al., 2015; Yang, 2016; Zhang et al., 2016;
65 Qu, 2018; Zhao, 2018; Beijing Ancient Architecture Research Institute, 2018; Ye and Zhang et al., 2019;
66 Liu, 2020; Shu, 2020; Wang et al., 2020; Zha, 2021; He, 2021; Zhang, 2022; Li, 2023; Wang, 2023; Wang
67 et al., 2024). There have been numerous studies on the biological weathering of rocks worldwide. Research
68 on Roman marble monuments has shown that dark spots indicate the presence of cyanobacteria. This
69 biological activity promotes particle detachment and accelerates weathering, leading to pit formation. In
70 Trajan's Forum, the estimated rate of pit formation is 1 millimeter every 40 years. To prevent biological
71 corrosion of limestone and marble monuments, the habitats and ecological needs of various microorganisms
72 must be considered (Danin and Caneva, 1990). Microorganisms can spontaneously remove particles from
73 stone surfaces, causing corrosion of building materials (Praderio, et al., 1993). Humid climates and air
74 pollution make biological corrosion more destructive (Warscheid, et al., 1996). Bryophytes can corrode
75 rock substrates through biogeochemical and biogeophysical mechanisms (Altieri and Ricci, 1997). Studies
76 on stone monuments from Angkor, Maya, and Inca civilizations have found lichens, cyanobacteria, fungi,
77 and bacteria to be ubiquitous. The main causes of stone erosion are organic and inorganic acids (sulfuric
78 and nitric acids) produced by microorganisms, as well as sulfur cycling and oxidation (Zhang et al., 2019).
79 Microbial communities form biofilms that cover the surface of building stones, adapting to the limited
80 nutrient and water conditions for growth. These biofilms create colored biological coatings that cause
81 aesthetic damage to the building stones and alter the structural properties of the materials. They can even
82 promote "non-biological" corrosion processes through mechanical pressure caused by the shrinking and
83 swelling of the colloidal biofilms, leading to further weakening of the mineral lattices. Acid decomposition
84 and redox biocorrosion processes result in the formation of harmful crusts on the building stones (Warscheid
85 and Braams, 2000). In the Yunnan Stone Forest of China, which consists of extremely pure carbonate rocks,



86 biological community corrosion can control the formation of some small-scale features (Tian et al., 2004).
87 A laboratory study using rock samples from Portugal showed that microalgae and cyanobacteria grow easily
88 on limestone but little to none on granite (Miller et al., 2006). A study of 249 samples from 83 different
89 locations in the Mediterranean found that cyanobacteria were the most common biocorrosion organisms
90 (Lombardozi et al., 2012). The Pyramid of Caius Cestius in Rome, a funeral building constructed between
91 272 and 279 CE, is covered with marble that has developed a gray-black microbial crust, primarily
92 consisting of spherical and filamentous cyanobacteria of the genera *Chroococcus*, *Gloeocapsa*, and
93 *Tolypothrix*, as well as green algae, fungi, and lichens (Golubić et al., 2015). Some researchers believe that
94 prokaryotes, fungi, micro-animals, and plants form an ecosystem that collectively participates in the
95 biocorrosion process of rocks (He et al., 2022). Microorganisms form a biofilm layer on rock surfaces. This
96 biofilm is a metabolic cooperative network that achieves optimal utilization and recycling of the substrate,
97 decaying plant and animal matter, animal feces, and other substances deposited from the atmosphere onto
98 the surface (Liu et al., 2022). Some researchers believe that cyanobacteria primarily corrode stone, while
99 bacteria, archaea, and fungi mainly corrode metals (Gaylarde and Little, 2022). Recent studies have found
100 high microbial diversity on marble surfaces, characterized mainly by cyanobacteria, proteobacteria, and
101 *Deinococcus-Thermus* (Timoncini, 2022).

102 This paper primarily analyzes the community composition, structure, and relative biomass of
103 biological communities on marble surfaces. It aims to identify the relationship between the distribution of
104 biological communities and the characteristics of marble surfaces, as well as to reveal the relationships and
105 mechanisms between the development process of biological communities and their biocorrosion processes.

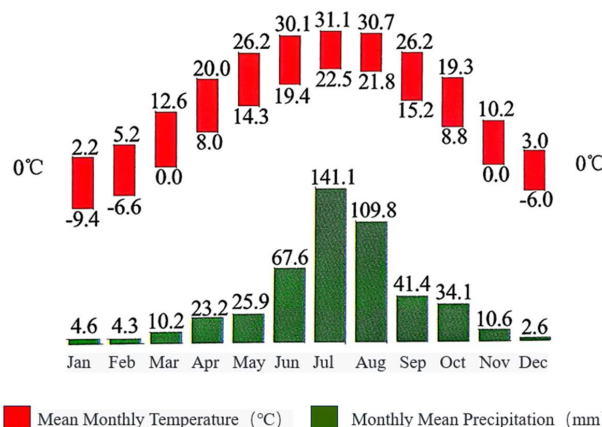
106

107 1 Overview of the Study Area

108 Beijing is located in a warm temperate semi-humid monsoon climate zone, characterized by a cool
109 mountainous climate. The average annual temperature in the region remains stable at 10.8°C, with a frost-
110 free period of approximately 150 days. In winter, Beijing is influenced by cold currents from the northwest,
111 resulting in a cold and dry climate with prevailing northwest winds and an average annual wind speed of
112 1.9 meters per second. During summer, the influence of tropical high-pressure systems leads to hot weather
113 with concentrated rainfall, particularly from July to September, which accounts for 85% of the annual
114 precipitation, often occurring as heavy rainstorms. Beijing typically experiences pleasant autumn weather,

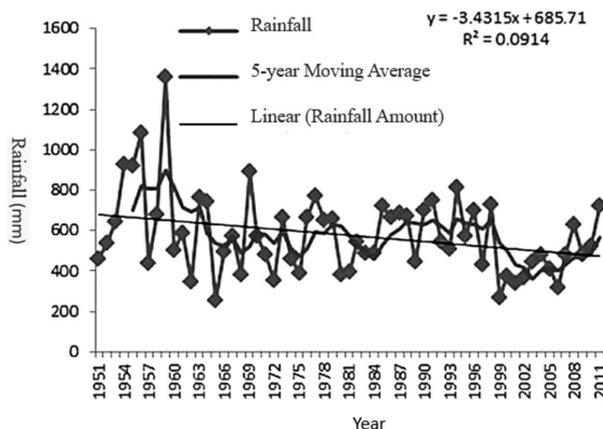


115 while spring is relatively short. The frost-free period ranges from 190 to 200 days. Under extreme weather
 116 conditions, summer temperatures can reach up to 42°C, while winter temperatures can drop to -25°C. The
 117 monthly average temperature and precipitation in Beijing from 1995 to 2015 are shown (Fig. 1) (Yang,
 118 2016). The annual precipitation in the Beijing area fluctuates significantly, ranging from 255.6 to 1316.3
 119 millimeters, with a multi-year average precipitation of approximately 579.3 millimeters. Through linear
 120 trend fitting observation, from 1951 to 2011, the precipitation shows a decreasing trend, with an average
 121 annual decrease of about 3.4 millimeters (Fig.2) (Li et al., 2014).



122
 123
 124

Fig. 1. Monthly average temperature and precipitation in Beijing, China from 1995 to 2015. (Yang, 2016)



125
 126
 127

Fig. 2. Interannual variation trend of precipitation in Beijing, China from 1951 to 2011. (Li et al., 2014)



128

129 The main production area of Beijing marble is Dashiwo Town, located in the southwestern part of
130 Fangshan District, Beijing. In Dashiwo Town, the blue-white stone was the earliest to be mined due to its
131 relatively shallow burial depth. The white marble, on the other hand, is buried deeper and is typically the
132 deepest layer among the stone strata, with a thickness ranging from 90cm to 150cm. In the construction
133 industry, both white marble and blue-white stone are widely used marble materials.

134

135 2 Research Methods

136 2.1 Field Work

137 Algal communities of different morphologies were collected from marble surfaces and placed in
138 specimen boxes. These were numbered, photographed, and their appearance, color, and morphology were
139 described, along with the date and location of collection. The micro-morphologies formed by the dissolution
140 of algal communities were observed and photographed. A total of 40 algal community specimens were
141 collected in the field, and 22 field photographs of algal communities were taken.

142

143 2.2 Laboratory Work

144 2.2.1. Microscopic Observation

145 A stereomicroscope (Szx7, Olympus, Japan) was used to observe the size, morphology, and color of
146 the algal communities. Then, temporary slides were prepared from algal communities of different colors
147 and observed under a biological microscope (Bx51, Olympus, Japan). The genera and species of algae were
148 identified (using reference books such as Desikachary, 1959; Geitler, 1932; Komarek, 1998; Zhu, 1991;
149 Fudi, 1980; Hu and Wei, 2006), and photographs were taken. In the laboratory, one microscope slide was
150 prepared for each lower plant ecological specimen number, totaling 40 lower plant microscope slides. A
151 total of 142 microscopic photographs were taken.

152 2.2.2. Biomass Statistics

153 The volume percentages of algae were recorded. These volume percentages were statistically analyzed
154 to calculate the relative volume (V_x , relative biomass). The statistical and calculation methods are as
155 follows:

156 (1) Relative Volume (V_x , Relative Biomass)



157 For each microscope slide, the percentage of volume occupied by each species of lower plant relative
158 to the total volume of lower plants on that slide was estimated (on the slide, the larger the area occupied by
159 a species of lower plant, the greater its volume). This gives the estimated volume percentage ($v(x)\%$) for
160 that species of lower plant on that slide. The volume percentages for the same species of lower plant across
161 all slides in the study area were then summed to obtain the relative volume for that species in the study area.
162 The relative volume of a lower plant reflects its relative biomass in the study area. It is not the actual volume
163 but is an estimated relative value, only meaningful for comparison purposes.

164
165
166

$$V_x = v(x)_{i_1} + v(x)_{i_2} + \dots + v(x)_{i_n}$$

167 i_n represents the microscope slide number; x represents a specific species of lower plant; $v(x)_{i_n}\%$
168 represents the estimated volume percentage of the lower plant x .

169

170 (2) Relative Volume Percentage (Y_x , Relative Biomass Percentage)

171 This is the percentage of the relative volume of one species of lower plant in relation to the sum of
172 relative volumes of all lower plants in the study area. It is also referred to as the relative biomass percentage.

173

$$174 Y_x = \frac{V_x}{n \times 100} \times 100\%$$

175

176 n represents the total number of microscope slides.

177

178 The relative volume percentage, also known as the relative biomass percentage, does not represent
179 the actual biomass. This is because it is currently very difficult to accurately measure the biomass of
180 microorganisms on marble surfaces. Through microscopic observation and estimation, we can roughly
181 understand the growth conditions of microorganisms. It is a relative value and only has comparative
182 significance.

183

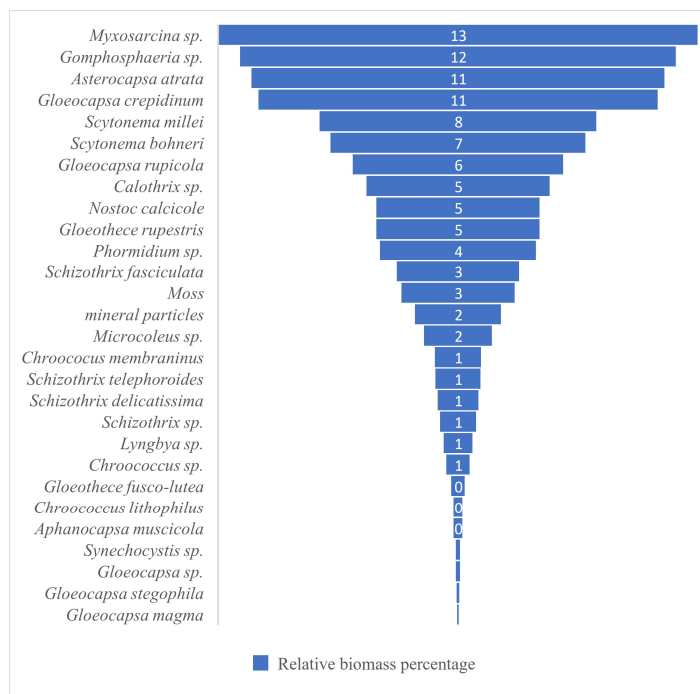
184 3 Results

185 3.1 Population Distribution Across the Entire Study Area



186

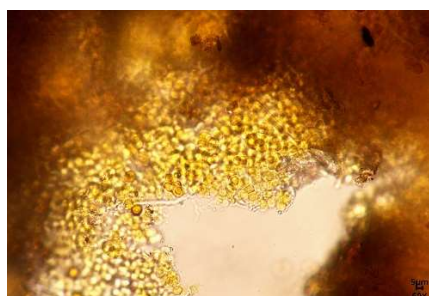
187 The biological composition on the marble surface in the study area is shown (Fig. 3). A total of 30
 188 genera and species were identified. The most abundant species is *Myxosarcina* sp., followed by
 189 *Gomphosphaeria* sp., *Asterocapsa atrata*, *Gloeocapsa crepidinum* (Fig. 4), and *Scytonema millei*, among
 190 others. These species are common aerophytic algae found on limestone rock surfaces (Tian et al. 2002,
 191 2003, and 2004). They thrive in calcareous environments, are drought-tolerant, grow slowly, and possess
 192 extremely strong vitality.



193

194 Fig. 3. Relative biomass percentage of marble surface in Beijing Temple of Heaven Park, Beijing, China.

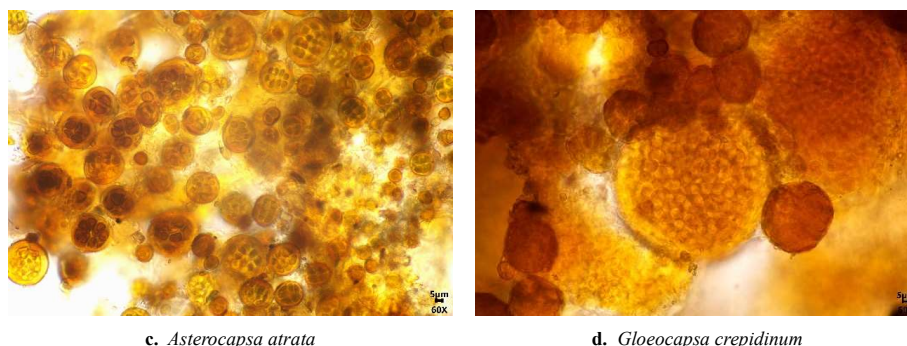
195



a. *Myxosarcina* sp.



b. *Gomphosphaeria* sp.



c. *Asterocapsa atrata*

d. *Gloeocapsa crepidinum*

196 **Fig. 4.** Dominant Organisms on the Marble Surface of the Temple of Heaven in Beijing, China.

197

198 3.2 Characteristics of Biological Population Distribution on Marble Surfaces with Different Orientations in the
199 Study Area

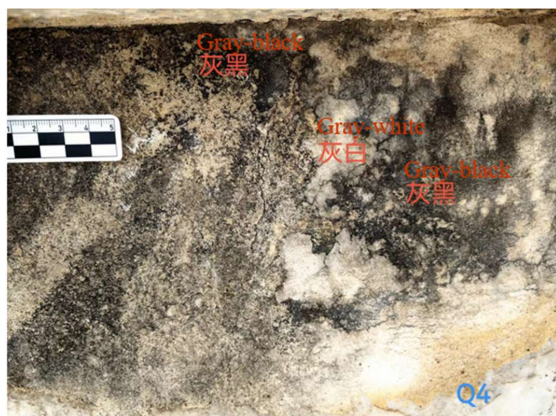
200 The Hall of Prayer for Good Harvests in the Temple of Heaven Park is a circular building. Marble surfaces
201 with different orientations receive varying amounts of sunlight exposure. The south-facing surface receives the
202 longest duration of sunlight, followed by the east and west-facing surfaces which receive half-day sunlight, while
203 the north-facing surface is shaded and receives no direct sunlight. This variation in sunlight exposure leads to
204 changes in the biological populations on the rock surfaces. The following sections will discuss these variations
205 separately:

206 3.2.1 Characteristics of Biological Populations on East-facing Rock Surfaces

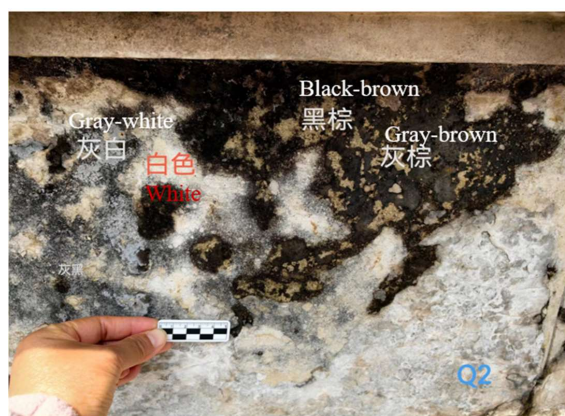
207 The biological communities on east-facing rock surfaces are primarily characterized by gray-white, gray-
208 brown, brown, gray-black, black-brown, white, and black-brown leathery appearances. The main species include
209 *Scytonema bohneri*, *Chlorococcum* sp., *Gloeocapsa rupestris*, *Gloeotheca rupestris*, *Myxosarcina* sp.,
210 *Phormidium* sp., *Calothrix* sp., *Gloeotheca crepidinum*, *Lyngbya* sp., *Gloeocapsa compacta*, and *Chroococcus*
211 *membraninus* (Fig.5) . Among these, the dominant species are *Scytonema bohneri* and *Chlorococcum* sp.,
212 accounting for 25% and 23% of the relative biomass percentage (Fig. 6) . *Scytonema* is a very common genus
213 among aerophytic algae (Tian et al. 2002, 2003, and 2004).

214

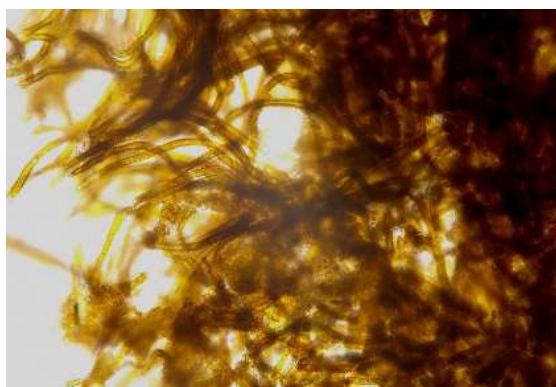
215



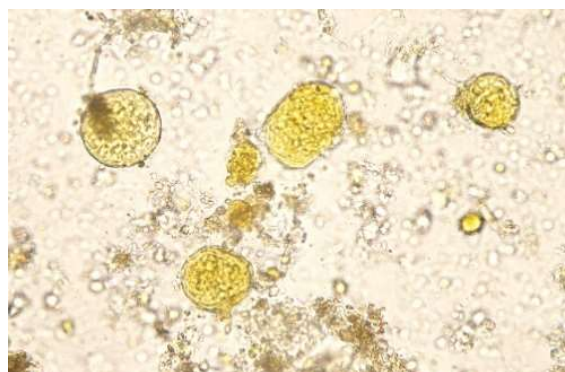
a. Gray-white, Gray-black



b. Gray-white, Gray-brown, Black-brown, White



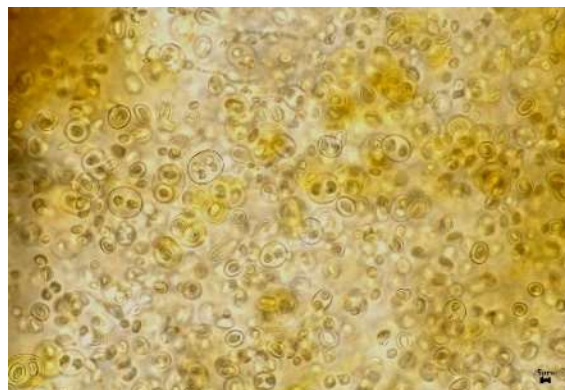
c. *Scytonema bohneri*



d. *Gomphosphaeria* sp.



e. *Gloeocapsa rupicola*



f. *Gloeothecae rupestris*

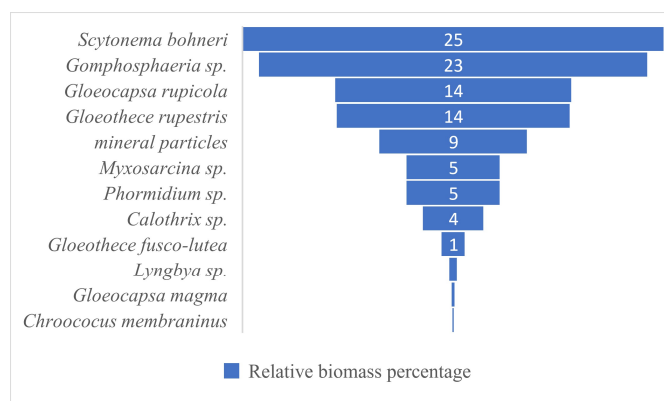
216 **Fig. 5.** Micrographs of biological communities and some species on the east-facing marble surface of Hall of Prayer for Good

217 Crops in Temple of Heaven Park, Beijing, China.

218



219



220

221 **Fig. 6.** Biological population relative biomass percentage on the east-facing marble surface of Hall of Prayer for Good Harvests
222 in Temple of Heaven Park, Beijing, China.

223

224 3.2.2 Characteristics of Biological Populations on West-facing Rock Surfaces

225 The biological communities on west-facing rock surfaces are primarily characterized by black hairy, black
226 membranous, yellow-green leathery, gray-black leathery, yellow-green, brown, and gray-green appearances. The
227 main species include *Scytonema millei*, mosses, *Schizothrix fasciculata*, *Myxosarcina sp.*, *Asterocapsa atrata*,
228 *Gloeocapsa crepidinum*, *Gomphosphaeria sp.*, and *Gloeocapsa rupicola* et al (Fig. 7) . Among these, the
229 dominant species are *Scytonema millei* and mosses et al, accounting for 28% and 20% of the relative biomass
230 percentage respectively (Fig. 8) .

231

232



a. Gray-black leathery



b. Black hairy and membranous



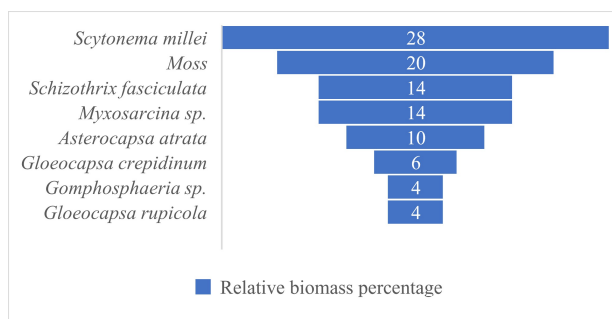
c. Yellow-green, Gray-green, Brown

d. *Scytonema millei*

e. moss

f. *Schizothrix fasciculata*

233 **Fig. 7.** Micrographs of biomes and some species on the west-facing marble surface of Hall of Prayer for Good Harvests in
 234 Temple of Heaven Park, Beijing, China.
 235
 236



237
 238 **Fig. 8.** Biological population relative biomass percentage on the west facing marble surface of Temple of Heaven Park, Beijing,
 239 China.
 240



241 3.2.3 Characteristics of Population Distribution on North-facing Surfaces

242 The biological communities on north-facing rock surfaces are primarily characterized by gray-brown
243 membranous, brown, gray-black, yellow-green, black-brown, gray-white, brown crusty, brown carpet-like,
244 brown-black leathery, and brown-black membranous appearances. The main species include *Myxosarcina* sp.,
245 *Gomphosphaeria* sp., *Gloeocapsa crepidinum*, *Schizothrix fasciculata*, *Asterocapsa atrata*, *Scytonema millei*,
246 *Calothrix* sp., mosses, *Gloeocapsa rupicola*, *Microcoleus* sp., *Chroococcus* sp., *Gloeotheca rupestris*, *Lyngbya*
247 sp., *Gloeocapsa* sp., *Scytonema bohneri*, and *Synechocystis* sp. et al (Fig. 9) . Among these, the dominant
248 species are *Myxosarcina* sp. and *Gomphosphaeria* sp., accounting for 17% and 15% of the relative biomass
249 percentage respectively (Fig. 10) .



a. Gray-brown membranous



b. Gray-black



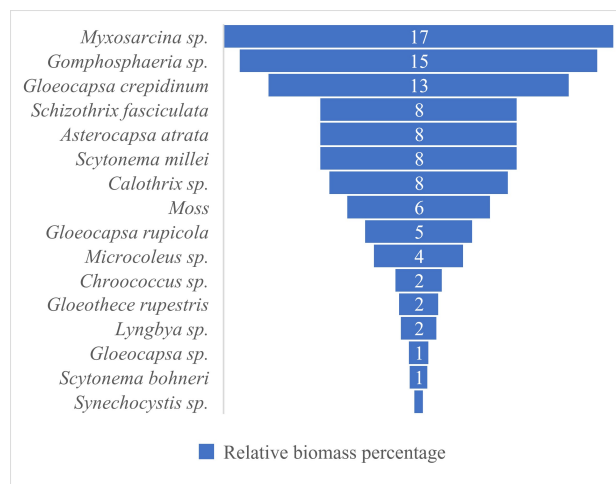
c. Yellow-green



d. Gray-white



250 **Fig. 9.** Micrograph of biological communities and some species on the north facing marble surface of Hall of Prayer for Good
 251 Harvests in Temple of Heaven Park, Beijing, China.
 252
 253



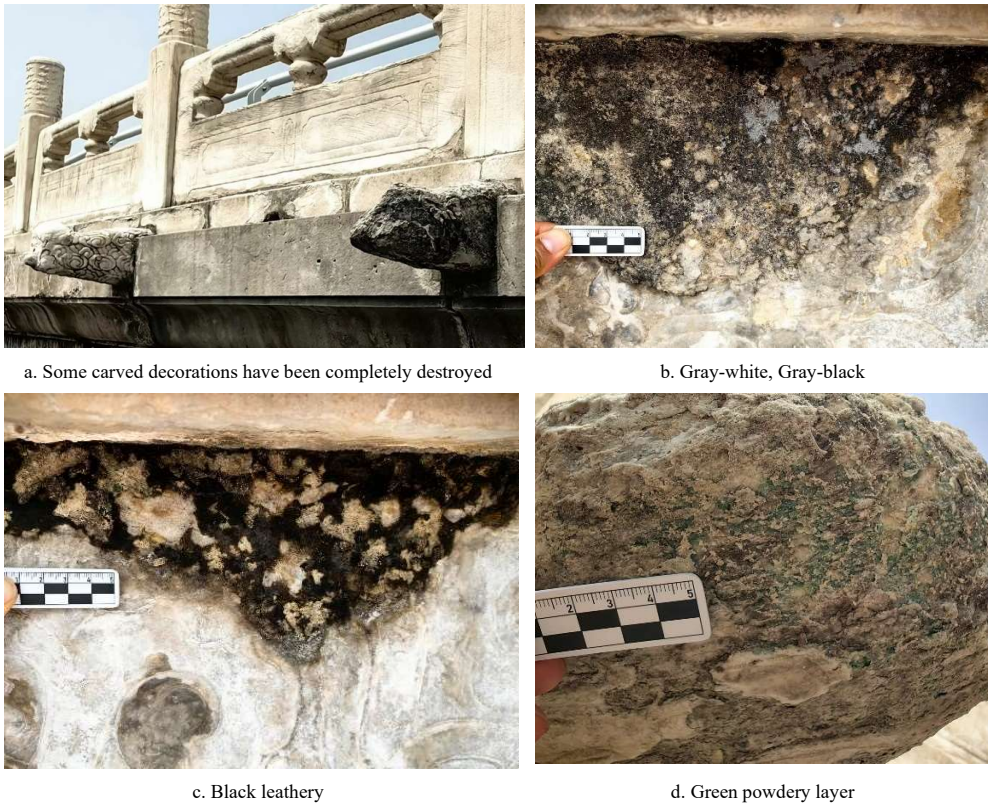
254
 255 **Fig. 10.** Relative biomass percentage of biological population on the north facing marble surface of Hall of Prayer for Good
 256 Harvests in Temple of Heaven Park, Beijing, China.
 257

258 3.2.4 Characteristics of Population Distribution on South-facing Surfaces

259 The biological communities on south-facing rock surfaces are primarily characterized by gray-green
 260 leathery, gray-white, gray-black membranous, black leathery, gray-black, brown-yellow, and green powdery
 261 layer appearances. The main species include *Scytonema millei*, *Nostoc calcicola*, *Asterocapsa atrata*,
 262 *Myxosarcina* sp., *Phormidium* sp., *Gloeocapsa crepidinum*, *Chroococcus membraninus*, *Schizothrix*



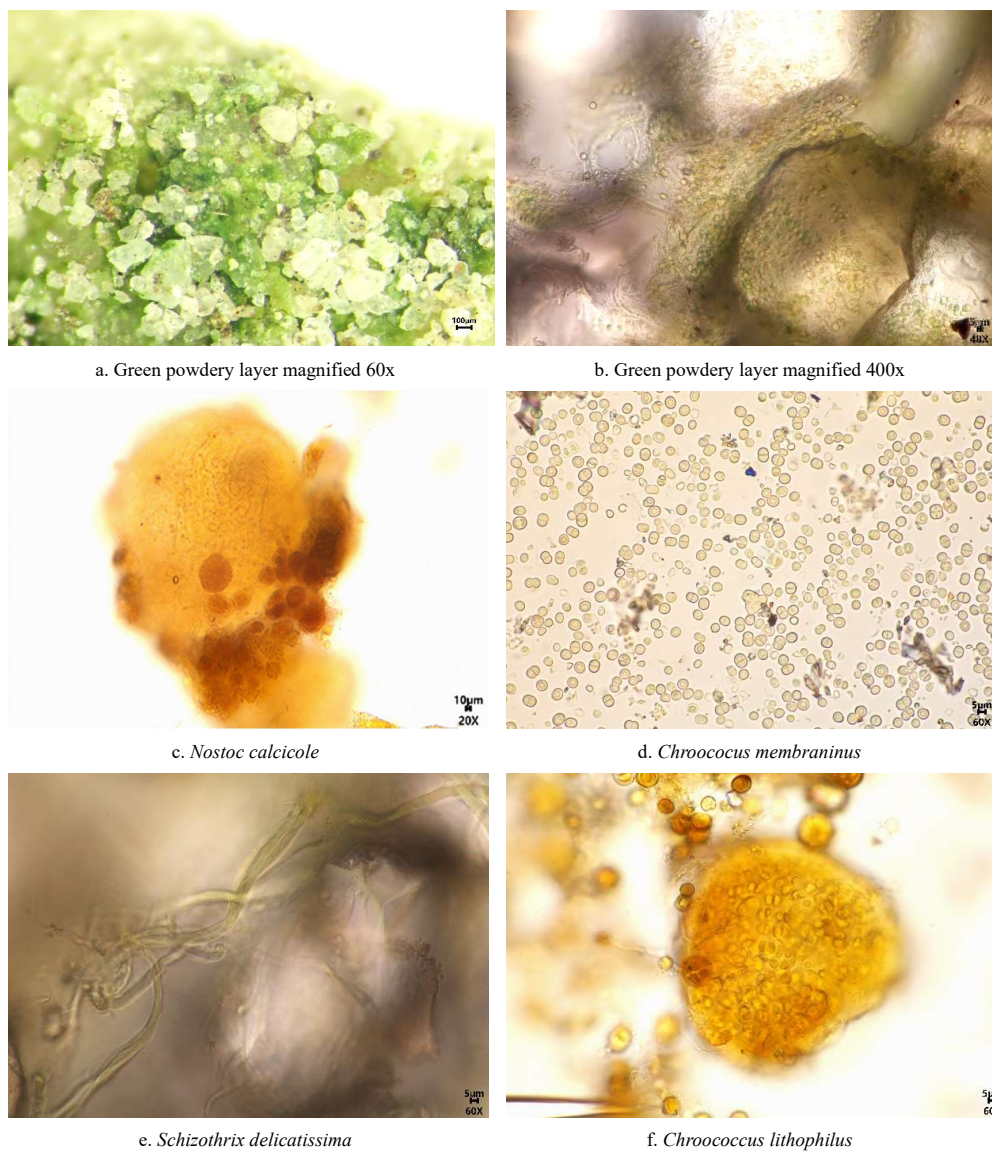
263 *delicatissima*, *Schizothrix* sp, *Microcoleus* sp., *Aphanocapsa muscicola*, *Chroococcus lithophilus*, *Lyngbya* sp.,
264 *Gloeocapsa* sp., and *Gloeocapsa sanguinea* et al (Fig. 11) . Among these, the dominant species are *Scytonema*
265 *millei* and *Nostoc calcicola*, accounting for 25% and 20% of the relative biomass percentage respectively (Fig.
266 12) .



267 **Fig. 11.** Field photo of biomes on the south facing marble surface of Hall of Prayer for Good Harvests in Temple of Heaven Park,
268 Beijing, China.

269

270



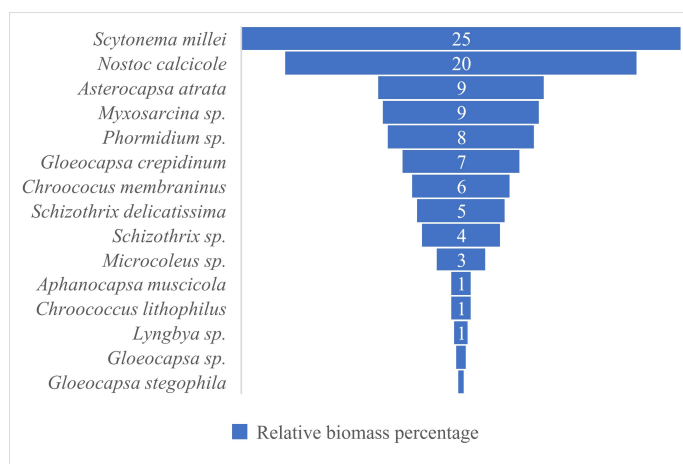
271 **Fig. 12.** Micrograph of biomes and some species on the south facing marble surface of Hall of Prayer for Good Harvests in

272 Temple of Heaven Park, Beijing, China.

273

274

275



276

277 **Fig. 13.** Biological population relative biomass percentage on the south facing marble surface of Hall of Prayer for Good

278 Harvests in Temple of Heaven Park, Beijing, China.

279

280 3.2.5 Comparison of Populations on Different Orientations

281 The main aerophytes algae on rock surfaces include spherical algae, small filamentous algae, and large
282 filamentous algae. Their distribution is primarily influenced by the substrate's looseness, sunlight, and moisture.
283 From spherical algae to small filamentous algae to large filamentous algae, they require increasingly loose
284 substrates, more moisture, and longer sunlight exposure (Table 1). Mosses generally prefer shaded and moist
285 environments.

286 Although the east and west sides of the Hall of Prayer for Good Harvests in the Temple of Heaven Park
287 receive sunlight for half a day each (Table 2), the eastern side receives sunlight in the morning when the rock
288 surface temperature is lower. Even with abundant sunlight, the algal growth on the eastern surface is not as good
289 as on the western side. The western side receives sunlight in the afternoon when the rock surface temperature is
290 higher, providing both water and heat conditions simultaneously, which is more conducive to algal growth. This
291 results in the appearance of *Scytonema millei*, the algae that prefers to grow on looser substrates, as well as more
292 moss plants, leading to more severe weathering on the western rock surface. The north-facing side is shaded,
293 with slower water evaporation, mainly supporting the growth of spherical algae, and experiencing relatively
294 weaker weathering. The south-facing side receives longer sunlight exposure and weathers faster, with the carved
295 patterns on the rock surface completely destroyed (Fig. 11a). The substrate has a high degree of looseness, even
296 allowing for the appearance of large filamentous algae like *Nostoc*. *Nostoc* typically prefers to live in soil rather



297 than on rock surfaces, indicating that the south-facing marble has weathered very severely, forming a loose, thick
 298 weathered layer similar to soil. However, mosses are not present on the south-facing side. This may be due to
 299 the long sunlight exposure on the south-facing side, which leads to rapid evaporation, causing the rock surface
 300 to become excessively dry.

301 The sensitivity of aerophytic algae to microenvironments is well revealed through the analysis of the
 302 composition of aerophytes populations on marble surfaces with different orientations of the Hall of Prayer for
 303 Good Harvests.

304

305 **Table 1**

306 Requirements of aerophyte growth on rock surface environment.

Epilithic Aerophytes	Rock Surface Substrate	Rock Surface Moisture	Rock Surface Sunlight
	Looseness		Duration
Spherical algae	compact ↓	dry ↓	less ↓
Small filamentous algae			
Large filamentous algae	loose ↓	wet ↓	more ↓
Mosses	Relatively loose, shaded and moist environment		

307

308 **Table 2**

309 Environmental characteristics and dominant species of marble surface of Hall of Prayer for Good Harvest in Temple of
 310 Heaven Park, Beijing, China.

Marble Surface Orientation	Sunlight	Moisture	Environmental Characteristics	Dominant Species
North-facing	None	Slow evaporation	Cold and humid	Spherical algae
East-facing	Half day	Rapid evaporation in the morning	Warm and humid	Small filamentous algae, Spherical algae
West-facing	Half day	Rapid evaporation in the afternoon	Hot and humid	Small filamentous algae, Mosses
South-facing	Full day	Rapid evaporation during the day	Hot and dry	Small filamentous algae, Large filamentous algae

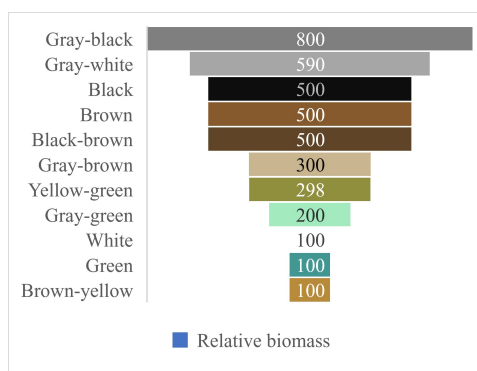
311

312 3.3 Relative Biomass of Different Colored Biological Communities on Rock Surfaces in the Study Area

313 The colors displayed by aerophytic algae and mosses on rock surfaces differ from those observed under a
 314 microscope. In this paper, the former is referred to as the "visual color," while the latter is called the "microscopic
 315 color." The visual color is the community color presented when different populations aggregate together, whereas
 316 the microscopic color is the color of different species observed under magnification through a microscope. Often,
 317 communities of algae with different microscopic colors appear mostly black or gray-black of visual color.



318 The visual colors of biological communities on rock surfaces in the study area can be categorized into gray-
319 black, gray-white, black, brown, black-brown, gray-brown, yellow-green, gray-green, white, green, and brown-
320 yellow. Their relative biomass is shown (Fig. 14). The most common color is gray-black, followed by gray-
321 white, black, brown, and black-brown. These are also typical colors exhibited by aerophytic cyanobacteria in the
322 field, sometimes referred to as "ink bands." For example, the Nine Horses Fresco Hill (Jiuma Huashan) in the
323 Guilin landscape of China is formed due to aerophytic cyanobacteria growing on the rocks, creating black ink-
324 like bands.



325
326 **Fig. 14.** Relative biomass of biomes with different colors on the marble surface of Hall of Prayer for Good Harvests in Temple of
327 Heaven Park, Beijing, China.

328

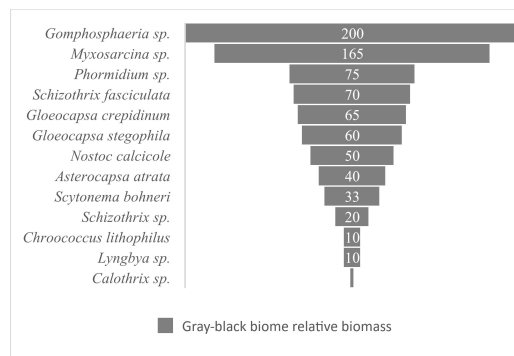
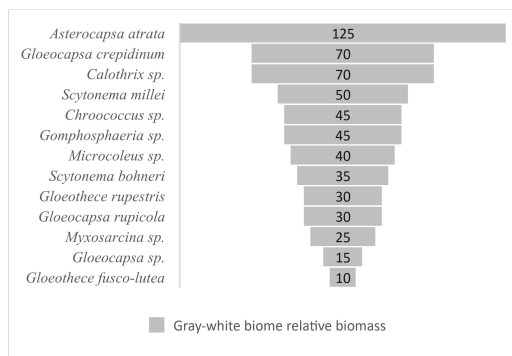
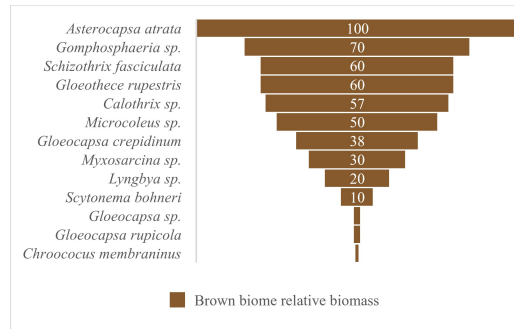
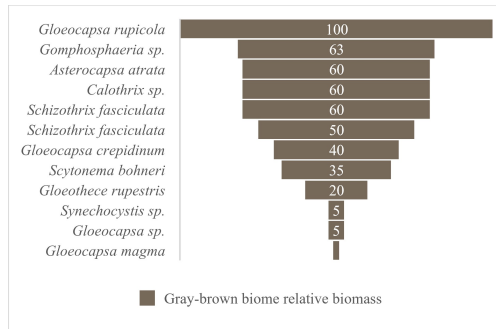
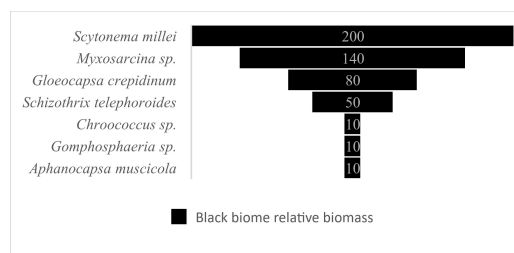
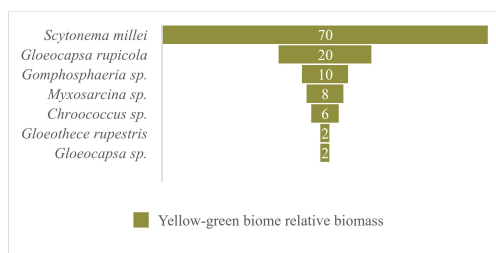
329 3.4 Relative Biomass of Population Composition in Different Colored Biological Communities on Rock 330 Surfaces in the Study Area

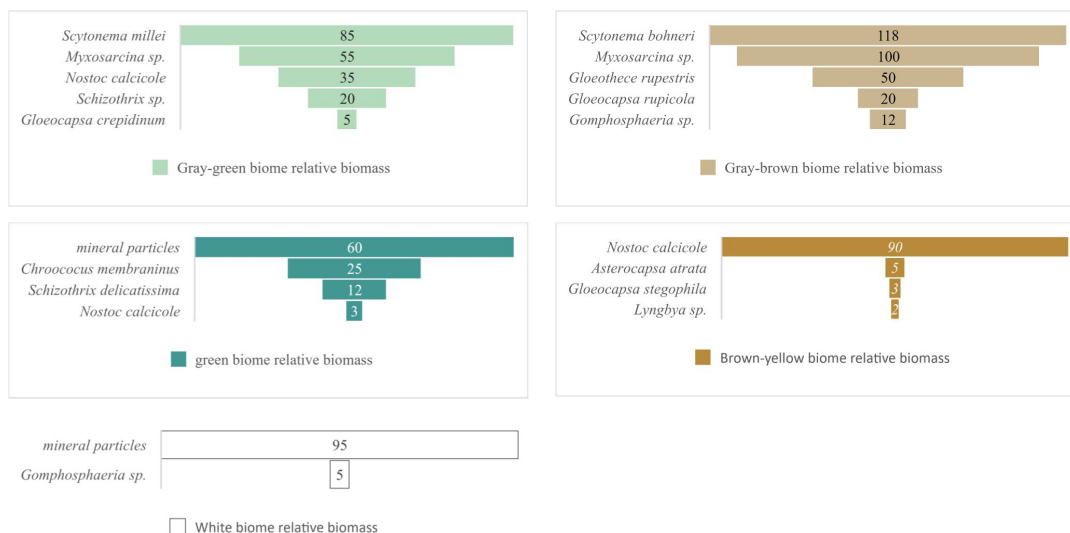
331 The relative biomass of population compositions in different visually colored biological communities on
332 rock surfaces in the study area is shown (Fig. 14). An analysis of the main population compositions of these
333 biological communities is presented (Fig. 15). The colors of biological communities on rock surfaces in the
334 study area are primarily composed of black, brown, gray, green, and yellow, as well as combinations of these
335 colors (gray-black, gray-white, black-brown, gray-brown, yellow-green, gray-green, and brown-yellow). The
336 correlation between color combinations and population composition is not very apparent, which also indicates
337 that determining microscopic color (population composition) through visual color is a complex and difficult
338 task. Nevertheless, some patterns can be observed:

339 1. Species like *Scytonema millei*, *Myxosarcina* sp., *Asterocapsa atrata*, *Gomphosphaeria* sp., and *Gloeocapsa*
340 *rupicola* tend to make the community color darker, presenting as black, brown, gray, or combinations of these.

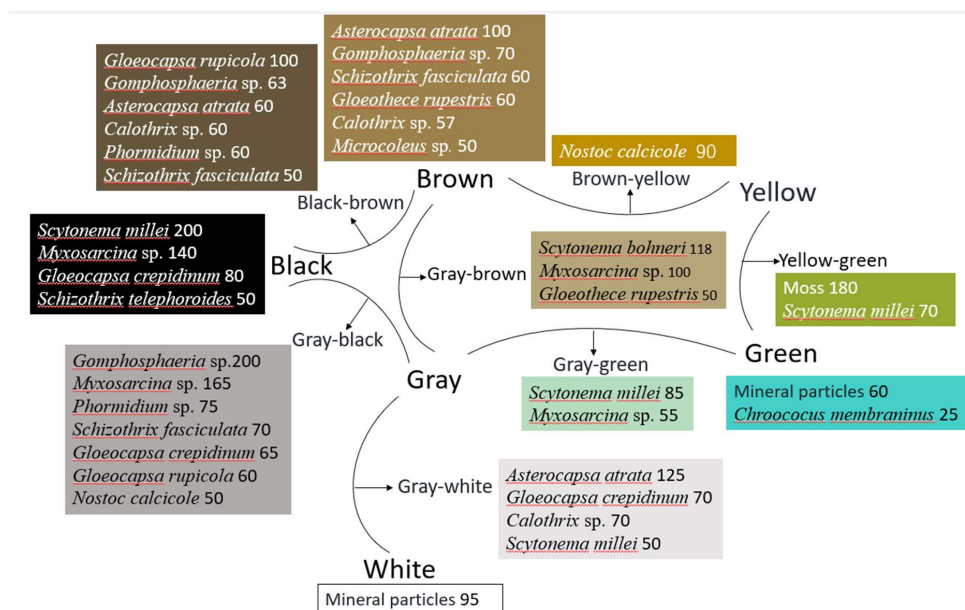


- 341 2. The white-colored areas observed visually are mineral particles, not biological, when viewed under a
 342 microscope.
 343 3. The visually green-colored areas (mainly referring to the unique blue-green color of cyanobacteria) are
 344 mineral particles and *Chroococcus membraninus*.
 345 4. The yellow-green visual color is mainly composed of mosses.
 346 5. The brown-yellow visual color is primarily composed of *Nostoc calcicole* etc.
 347





348 **Fig. 15.** Relative biomass of community composition of different colors on marble surface of Hall of Prayer for Good Harvests in
 349 Temple of Heaven Park, Beijing, China.
 350

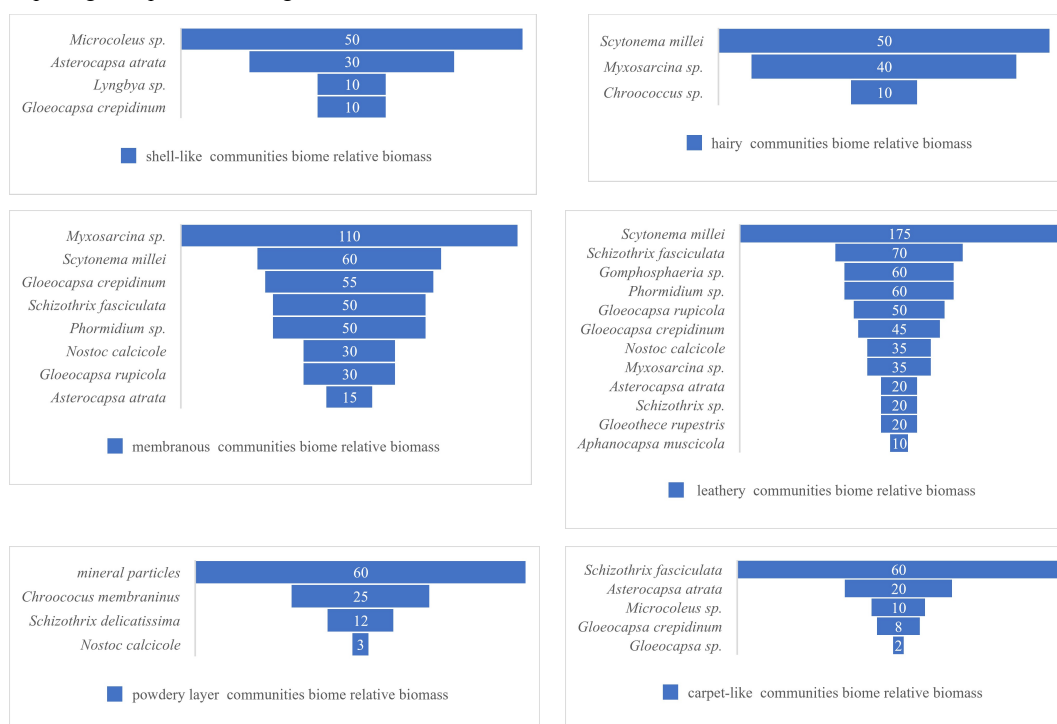


351
 352 **Fig. 16.** Analysis of main population composition of different color biomes on marble surface of Hall of Prayer for Good
 353 Harvests in Temple of Heaven Park, Beijing, China.

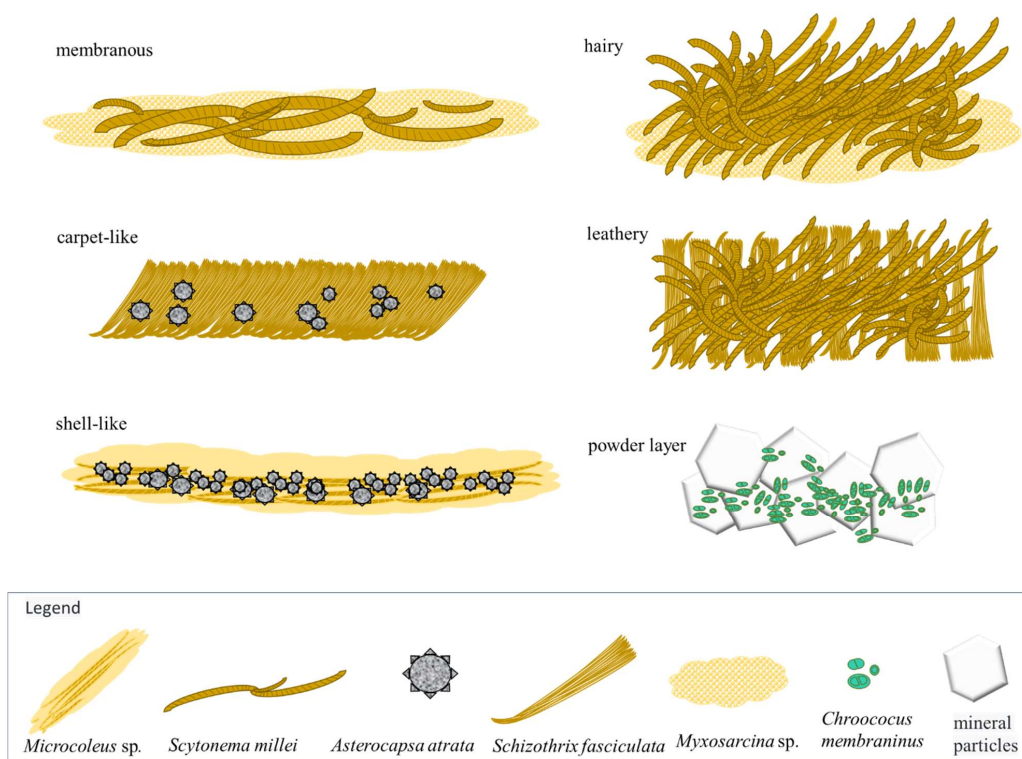


354 3.5 Relative Biomass of Population Composition in Different Morphological Biological Communities on Rock
 355 Surfaces in the Study Area

356 The biological communities on rock surfaces in the study area exhibit different morphologies, including
 357 membranous, hairy, carpet-like, leathery, shell-like, and powdery layers. Their relative biomass of population
 358 composition is shown (Fig. 17). A diagrammatic explanation of the formation of these community
 359 morphologies is presented (Fig. 18).



360 **Fig. 17.** Relative biomass of different forms of community on marble surface of Hall of Prayer for Good Harvests in Temple of
 361 Heaven Park, Beijing, China.
 362



363

364 **Fig. 18.** Morphological genesis diagram of different communities on marble surface of Hall of Prayer for Good Harvests in
 365 Temple of Heaven Park, Beijing, China.

366

367 The dominant species in the membranous biological communities are mainly *Myxosarcina* sp. and
 368 *Scytonema millei*. The former accounts for a relative biomass of 110, while the latter accounts for 60 (Fig. 17) .
 369 *Myxosarcina* sp. is a spherical alga (Fig. 4a) . It has thick individual sheaths, forming a dense colonial
 370 mucilage. *Scytonema millei* grows interspersed within, forming a membrane-like community (Fig.18) . When
 371 the relative biomass of *Scytonema millei* in the community exceeds that of *Myxosarcina* sp., it forms a hairy
 372 community (Fig. 18) . The dominant species in the carpet-like communities are mainly *Schizothrix fasciculata*
 373 and *Asterocapsa atrata*. The former accounts for a relative biomass of 60, while the latter accounts for 20 (Fig.
 374 17) . *Schizothrix fasciculata* grows densely together, forming a carpet-like structure (Figure 18) . The
 375 dominant species in the leathery biological communities are mainly *Scytonema millei* and *Schizothrix fasciculata*.
 376 The former accounts for a relative biomass of 175, while the latter accounts for 70 (Fig. 17) . *Scytonema millei*
 377 intertwines, with *Schizothrix fasciculata* interspersed within (Fig. 18) . The dominant species in the shell-like



378 biological communities are mainly *Microcoleus* sp. and *Asterocapsa atrata*. The former accounts for a relative
379 biomass of 50, while the latter accounts for 30 (Fig. 17) . *Microcoleus* sp. has well-developed sheaths, with
380 multiple algal filaments inside each sheath. The sheaths of multiple *Microcoleus* sp. aggregate to form a
381 mucilaginous layer, with *Asterocapsa atrata* dispersed within. When the mucilaginous layer dries, it cracks into
382 numerous small pieces. The edges of each piece detach from the rock surface and curl up, forming a shell-like
383 structure (Fig. 18 and Fig. 19) . The powder layer is a severely weathered surface (Fig. 11d) . Under
384 microscopic observation, it mainly consists of mineral particles and *Chroococcus membraninus*, with the former
385 accounting for 60 and the latter for 20 of the relative quantity (Fig. 17) . *Chroococcus membraninus* is
386 distributed on the surface and in the crevices of mineral particles (Fig. 12a and b) . The color of the community
387 appears as a mixture of the green color of *Chroococcus membraninus* (or the blue-green color characteristic of
388 cyanobacteria) and the white color of mineral particles.

389

390 3.6 Biological Weathering on Rock Surfaces in the Study Area

391 The growth distribution of aerophytes on rock surfaces in the study area is closely related to the surface
392 smoothness and texture of marble (Table 3). If the marble surface is uneven or has a non-uniform texture, the
393 aerophytes communities will be distributed in a spotted pattern (Fig. 19a). Dissolution forms solution pits and
394 cavities (Fig. 19b), which further expand into solution basins (Fig. 19c, d). If the marble surface has linear
395 textures or non-uniform texture with joint stripes, the aerophytes communities will be distributed in a linear
396 pattern (Fig. 19e). Dissolution forms solution marks and grooves (Fig.19f), which further expand into solution
397 channels (Fig. 19g). If the marble surface is smooth and has a uniform texture, the aerophytes communities will
398 be distributed in a planar pattern (Fig. 19h). Dissolution forms a weathering layer or exfoliation layer (Fig. 19i).
399 Some studies also suggest that the type of stone, its position on the building, and the surface roughness of the
400 stone greatly influence biological growth (Korkanç and Savran, 2015).

401

402

403

404

405

406



407

408

409

410

Table 3

Characteristics of marble in Temple of Heaven Park, Beijing, China. and the process of biological corrosion on its surface.

Marble Characteristics	Biological Community Distribution	Resulting Dissolution Forms	Development Process
Uneven surface or non-uniform texture	Spotted distribution	Solution pits, cavities, and basins	↓
Surface with linear textures or non-uniform texture with joint stripes	Linear distribution	Solution marks, grooves, and channels	
Smooth surface with uniform texture	Areal distribution	Weathering layer, exfoliation layer	

411

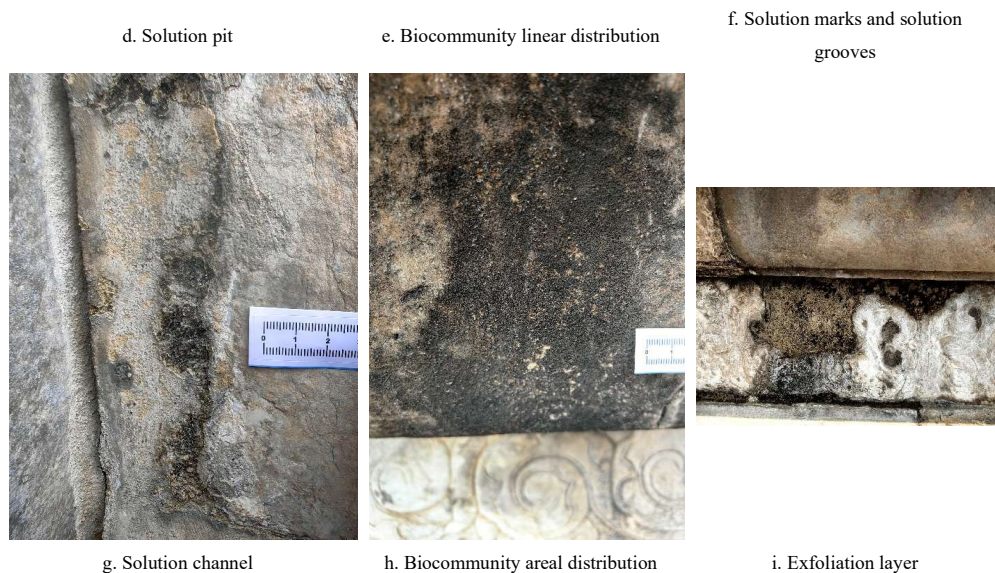
412



a. Biocommunity point distribution

b. Solution pores and solution cavities

c. Sinkhole



413 **Fig. 19.** Biological weathering forms on the marble surface of Hall of Prayer for Good Harvests in Temple of Heaven Park,
414 Beijing, China.

415

416 The spotted distribution of biological communities gradually expands into linear distribution, and then into
417 planar distribution. Solution pits, basins, and cavities also further enlarge their dissolution forms, developing
418 into solution marks, grooves, and channels. For example, in the weathering process of the cloud-patterned white
419 marble water spouts on the Hall of Prayer for Good Harvests in the study area, biological communities first
420 accumulate and grow in the depressions of the patterns (Fig. 20a, b). These areas retain more moisture, so they
421 are the first to undergo biological weathering, forming deeper solution cavities and channels. The communities
422 then gradually spread to the surrounding areas, developing into linear distributions, and then areal distributions,
423 leading to flaking of the rock surface (Fig. 20c). This partially destroys the pattern structure, further expanding
424 the area and depth of dissolution, forming a loose powder layer (Fig. 11a, d, Fig. 12a, b, Fig. 20d, e, f).

425



a. Organisms gather and grow in the depressions of the patterns



b. Organisms gather and grow in the depressions of the patterns



c. Flaky exfoliation on the surface of the emerging cloud-like decorations



d. Some emerging cloud-like decorations are structurally damaged



e. Emerging cloud-like decorations have weathered almost completely



f. Emerging cloud-like decorations form a loose powdery layer

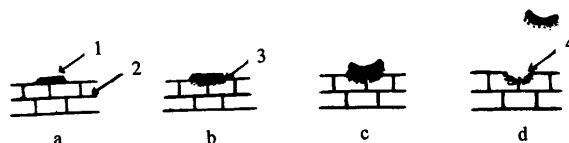
426 **Fig. 20.** Biological weathering process of the emerging cloud-like marble decorations on the Hall of Prayer for Good Harvests in
427 Temple of Heaven Park, Beijing, China.

428
429

430 The dissolution mechanism of aerophytes communities on rocks in the study area primarily involves the
431 organisms' attempt to obtain inorganic nutrients such as calcium and magnesium ions from the rock. These
432 aerophytes communities can secrete organic acids, which release calcium and magnesium ions from the rock,
433 thereby obtaining inorganic nutrients for their growth and development. Through this acid erosion process,
434 aerophytes communities can "eat away" at the rock, forming tiny hemispherical dissolution pits (Fig. 21), thus
435 damaging the surface structure of the rock and forming an underlying weathering layer (Tian et al., 2004).

436
437

438





439

440 **Fig. 21.** Schematic diagram of the formation of hemispherical small-scale dissolution forms in Yunnan Stone Forest, China.

441 1. Cyanobacterial crust; 2. Carbonate rock; 3. Underlying weathering layer; 4. Hemispherical dissolution morphology. a. Shell-
442 like, membrane-like and other cyanobacterial communities attach to the surface of carbonate rocks; b. The cyanobacterial
443 communities exert long-term biodissolution effects on the underlying rock, forming an underlying weathering layer; c. During
444 dry climate conditions, the algal crust contracts, and the edges of the crust gradually detach from the rock surface; d. As the algal
445 crust further dries and shrinks, under external forces (such as wind), it completely detaches from the rock surface. Due to the
446 adhesive nature of the algal crust, the detached crust carries away some of the white powder from the underlying weathering
447 layer, leaving behind a hemispherical dissolution morphology at that location. (Tian et al., 2004)

448

449 4 Discussion

450 This study primarily focuses on algae and mosses visible under biological microscopes and does
451 not address other bacteria. Whether other bacteria are present is a matter that requires further
452 verification and in-depth research in the future.

453 Detailed investigation and research on biological communities on marble surfaces help reveal the
454 mechanisms and processes of biological weathering of marble artifacts. This can lead to more targeted
455 scientific methods for protecting marble cultural relics. The weathering of marble cultural relics in the
456 Temple of Heaven Park is due to physical, chemical, and biological factors. However, in many cases,
457 biological factors are the most destructive protagonists. They often form biofilms on marble surfaces,
458 corroding stone cultural relics over large areas, continuously damaging rocks through biophysical and
459 biochemical means.

460 Connections and issues between different research levels, methods, and results in this paper. This
461 paper studies the aerophytes on rock surfaces in the research area in terms of biological community
462 population composition, community color and morphology, and community distribution characteristics
463 (Table 4). The spotted, linear, and planar distributions of biological communities on rock surfaces in
464 the study area are composed of many microcommunities. These microcommunities exhibit different
465 morphologies, including membranous, hairy, carpet-like, leathery, shell-like, and powder layers.
466 Spotted, linear, and areal distributions of biological communities may be composed of one type of
467 microcommunity or multiple types. Microcommunities are further composed of multiple populations,



468 and a population consists of multiple individual organisms of the same species. Community distribution
 469 characteristics are observed with the naked eye, without magnification. Community color and shape
 470 are observed through stereomicroscopes and the naked eye, magnifying objects 8-56 times (or no
 471 magnification if observed with the naked eye). Biological community population composition is
 472 identified through biological microscope observation, magnifying objects 40-1000 times. This
 473 represents three stages of research with increasing magnification of the research object: 1) Distribution
 474 area; 2) Community; 3) Population. Research at each stage is relatively easy to conduct, but the
 475 connections between stages are challenging and represent a weakness in this paper. For example, to
 476 accurately correlate different colored and shaped communities with their precise population
 477 compositions (i.e., connecting the community stage with the population stage) requires statistical
 478 analysis of numerous specimens to improve accuracy. For instance, the observation of communities in
 479 outdoor settings, specifically the transition between distribution stages and community stages,
 480 primarily relies on the naked eye. Only a small number of observations are performed using
 481 stereomicroscopes, as detailed stereomicroscopic observations requiring photographs must be
 482 conducted indoors. The sampling of cultural relics in scenic areas is extremely limited and must be
 483 carried out without damaging the relics. To address this issue, one approach is to enhance the
 484 performance of observation equipment to allow for in situ biological community observations outdoors
 485 without sampling, or to perform minimal sampling without damaging the relics.

486

487 **Table 4**

488 Analysis of the stages in biological weathering research on aerophytes on marble in the temple of heaven park, Beijing, China.

Research Level	Distribution Area	Community	Population
Observation Method	Naked eye	Stereomicroscope, naked eye	Biological microscope
Magnification	0	8-56, 0	40-1000
Classification	3 distribution characteristics (point, linear, and areal distribution)	11 colors: gray-black, gray-white, black, brown, black-brown, gray-brown, yellow-green, gray-green, white, green, brown-yellow	30 genera and species : <i>Myxosarcina</i> sp., <i>Gomphosphaeria</i> sp., <i>Asterocapsa atrata</i> and so on (Fig.3)
Composition	Composed of multiple communities	6 morphologies: membranous, hairy, carpet-like, leathery, shell-like, and powder layer	Composed of multiple individuals of a single species



489 5 Conclusion

490 The most dominant species on marble surfaces in the study area is *Myxosarcina* sp., followed by
491 *Gomphosphaeria* sp., *Asterocapsa atrata*, *Gloeocapsa crepidinum*, and *Scytonema millei*. These aerobic algae
492 prefer calcareous environments, are drought-tolerant, slow-growing, and extremely resilient. The biological
493 population composition on marble surfaces facing different directions at the Hall of Prayer for Good Harvests
494 in the Temple of Heaven Park varies due to differences in sunlight exposure. The east-facing side, warm and
495 humid, mainly hosts small filamentous and spherical algae such as *Scytonema millei* and *Gomphosphaeria* sp.
496 The west-facing side, hot and humid, primarily features *Scytonema millei* and mosses, with *Scytonema millei*
497 being a small filamentous alga. The north-facing side, cold and humid, mainly supports spherical algae like
498 *Myxosarcina* sp. and *Gomphosphaeria* sp. The south-facing side, hot and dry, primarily hosts small or large
499 filamentous algae such as *Scytonema millei* and *Nostoc calcicole*. Rock surface biological communities in the
500 study area display various colors, with gray-black being the most common, followed by gray-white, black, brown,
501 and brown-black. Gray-black communities are mainly composed of *Myxosarcina* sp. and *Gomphosphaeria* sp.
502 Rock surface biological communities in the study area exhibit different morphologies, including membranous,
503 hairy, carpet-like, leathery, shell-like, and powder layers. Different morphologies correspond to different
504 population compositions. The growth and distribution of aerophytes on rock surfaces in the study area are closely
505 related to the smoothness and texture of the marble surface. Where the marble surface is uneven or has
506 inconsistent texture, aerophytes communities show a spotted distribution, forming dissolution holes, cavities,
507 and pits. Where the marble surface has linear patterns or uneven texture with joint stripes, aerophytes
508 communities display a linear distribution, forming dissolution marks, grooves, and channels. Where the marble
509 surface is smooth with uniform texture, aerophytes communities exhibit an areal distribution, forming
510 weathering or exfoliation layers. The mechanism of biological dissolution involves aerophytes secreting organic
511 acids, which dissolve inorganic salts from the rock to obtain nutrients, thereby "eating away" at the rock,
512 damaging its surface structure, and gradually weathering the rock. Aerophytes grow abundantly on marble
513 surfaces. Finding ways to prevent or reduce the growth of these organisms is key to slowing down the weathering
514 process of stone cultural relics in the Temple of Heaven Park.

515

516 **Author contributions**

517 YT completed all the work on the paper, including sampling, photography, experimental data analysis, charting,



518 drawing, and writing the paper, among other tasks.

519

520 **Competing interests**

521 The author has declared that there are no competing interests.

522

523 **Acknowledgement**

524 This study was supported by National Science Foundation of China (Grant No. 40872197) and the Development

525 Fund of China University of Geosciences (Beijing) (Grant No. F02114).

526

527 **References**

528 Altieri, A, Ricci, S.: Calcium uptake in mosses and its role in stone biodeterioration. *International*

529 *Biodeterioration & Biodegradation*, 40(2): 201-204. [https://doi.org/10.1016/S0964-8305\(97\)00047-4](https://doi.org/10.1016/S0964-8305(97)00047-4),

530 1997.

531 Beijing Institute of Ancient Architecture.: *Research and Application of Stone Structure Protection in Ancient*

532 *Buildings in Beijing*. Beijing: China Literature and History Press. 1-330, 2018.

533 Cha, J. :The weathering process and protection materials of stone relics Lingyan Temple, Changqing, Shandong.

534 *Doctoral Dissertation*. Beijing: University of Science and Technology Beijing. 1-175.

535 <https://link.cnki.net/doi/10.26945/d.cnki.gbjku.2021.000387> , 2021.

536 Danin, A, Caneva, G.: Deterioration of limestone walls in Jerusalem and marble monuments in Rome caused by

537 cyanobacteria and cyanophilous lichens. *International Biodeterioration*, 26(6): 397-417.

538 [https://doi.org/10.1016/0265-3036\(90\)90004-Q](https://doi.org/10.1016/0265-3036(90)90004-Q), 1990.

539 Desikachary, T. V.: *Cyanophyta*. Indian Council of Agricultural Research. New Delhi.1~669.

540 <https://doi.org/10.1086/403350>, 1959.

541 Fott, B. (Translated by Luo,d.): *Phycology*. Shanghai: Shanghai Science and Technology Press. 11-396, 1980.

542 Gaylarde, C., Little B.: Biodeterioration of stone and metal — Fundamental microbial cycling processes with

543 spatial and temporal scale differences. *Science of The Total Environment*, 823: 153-193.

544 <https://doi.org/10.1016/j.scitotenv.2022.153193>, 2022.

545 Geitler, L.: *Cyanophyceae*. In L.Rabenhorst'S *Kryptogamen-Flora*, Band 14. Leipzig, Germany: Akademische

546 Verlagsgesellschaft m.b.H..1~1194, 1932.



- 547 Golubić, S., Pietrini, A. M., Ricci, S.: Euendolithic activity of the cyanobacterium *Chroococcus lithophilus* Erc.
548 In biodeterioration of the Pyramid of Caius Cestius, Rome, Italy. *International Biodeterioration &*
549 *Biodegradation*, 100: 7-16. <https://doi.org/10.1016/j.ibiod.2015.01.019>, 2015.
- 550 He, H.: Study on the Weathering of Marble Jinshi Steles in Beijing Confucius Temple. *Capital Museum Forum*,
551 (35): 226-231, 2021.
- 552 He, J., Zhang, N., Muhammad, A., Shen, X., Sun, C., Li, Q., et al.: From surviving to thriving, the assembly
553 processes of microbial communities in stone biodeterioration: A case study of the West Lake UNESCO
554 World Heritage area in China. *Science of The Total Environment*, 805: 1-15.
555 <https://doi.org/10.1016/j.scitotenv.2021.150395>, 2022.
- 556 Hu, H., Wei, Y. (Editors): *Systematics, Classification, and Ecology of Freshwater Algae in China*. Beijing:
557 Science Press. 23-203, 2006.
- 558 Komarek, J. And Anagnostidis, K.: Cyanoprokaryota 1. Teil: Chroococcales. Vol. 19(1), In: Ettl H., Gaertner G,
559 Heynig, H. and Mollenhauer, D. (eds.), *Suesswasserflora von Mitteleuropa*, Gustav Fischer, Jena-Stuttgart-
560 Luebeck:Ulm. 1-548. <https://doi.org/10.2216/i0031-8884-38-6-544.1>, 1998.
- 561 Korkanç, M., Savran, A.: Impact of the surface roughness of stones used in historical buildings on
562 biodeterioration. *Construction and Building Materials*, 80: 279-294.
563 <https://doi.org/10.1016/j.conbuildmat.2015.01.073>, 2015.
- 564 Li, H., Deng, W., Yu, X.: Analysis of Precipitation Characteristics in Beijing Area from 1951 to 2011. *Inner*
565 *Mongolia Water Resources*, (02): 57-58, 2014.
- 566 Li, J.: Research on mechanical properties evaluation and deterioration mechanism of heritage rock in different
567 environment. Master's Thesis. Beijing: Beijing University of Civil Engineering and Architecture. 1-72.
568 <https://link.cnki.net/doi/10.26943/d.cnki.gbjzc.2023.000478>, 2023.
- 569 Liu, J.: Experimental study of thermal effects on Physical-mechanical properties of Beijing dolomitic marble.
570 Master's Thesis. Beijing: China University of Geosciences (Beijing). 1-78.
571 <https://link.cnki.net/doi/10.27493/d.cnki.gzdzzy.2020.001911>, 2020.
- 572 Liu, Q.: Biomimetic conservation of historic stones inspired by biomineralization. Doctoral Dissertation. Hangzhou:
573 Zhejiang University. 1-159, 2007.
- 574 Liu, Q., Zhang, B., Long, M.: Study on the Side Effects of Chemical Protection on the Surface of Stone Cultural
575 Relics. *Proceedings of the 2005 Yungang International Academic Symposium (Conservation Volume)*. 280-



- 576 286, 2005.
- 577 Liu, Q., Zhang, B., Long, M.: The harmful effects of surface chemical protection of historic stones. *Sciences of*
578 *Conservation and Archaeology*, (02): 1-7. [https://link.cnki.net/doi/10.16334/j.cnki.cn31-](https://link.cnki.net/doi/10.16334/j.cnki.cn31-1652/k.2006.02.001)
579 [1652/k.2006.02.001](https://link.cnki.net/doi/10.16334/j.cnki.cn31-1652/k.2006.02.001), 2006.
- 580 Liu, X., Qian, Y., Wu, F., Wang, Y., Wang, W., Gu, J.: Biofilms on stone monuments: biodeterioration or
581 bioprotection? *Trends in Microbiology*, 30(9): 816-819. <https://doi.org/10.1016/j.tim.2022.05.012>, 2022. a
- 582 Lombardozi, V., Castrignanò, T., DAntonio, M., Casanova Municchia, A., Caneva, G.: An interactive database
583 for an ecological analysis of stone biopitting. *International Biodeterioration & Biodegradation*, 73: 8-15.
584 <https://doi.org/10.1016/j.ibiod.2012.04.016>, 2012.
- 585 Lv, J., Wei, J.: Contribution of Dashiwo Marble in Fangshan, Beijing to the Foundation of the Forbidden City
586 and Stone Sutras of Yunju Temple. *Fossil*, (03): 68-73, 2020.
- 587 Miller, A., Dionisio, A., Macedo, M. F.: Primary bioreceptivity: A comparative study of different Portuguese
588 lithotypes. *International Biodeterioration & Biodegradation*, 57(2): 136-142.
589 <https://doi.org/10.1016/j.ibiod.2006.01.003>, 2006.
- 590 Praderio, G., Schiraldi, A., Sorlini, C., Stassi, A., Zanardini, E.: Microbiological and calorimetric investigations
591 on degraded marbles from the Cà d'Oro facade (Venice). *Thermochimica Acta*, 227: 205-213.
592 [https://doi.org/10.1016/0040-6031\(93\)80263-A](https://doi.org/10.1016/0040-6031(93)80263-A), 1993.
- 593 Qu, S.: The research on the weathering mechanism and weathering degree evaluation system of marble relics in
594 Beijing. Master's Thesis. Beijing: Beijing University of Chemical Technology. 1-140, 2018.
- 595 Shu, H.: Study on the Protection of Stone Cultural Relics by TiO₂ Modified Sol. Master's Thesis. Kunming:
596 Yunnan University. 1-72. <https://link.cnki.net/doi/10.27456/d.cnki.gyndu.2020.001939>, 2020.
- 597 Tian, Y., Zhang, J., Song, L., Bao, H.: A Study on Aerial Cyanophyta (Cyanobacteria) on the Surface of
598 Carbonate Rock in Yunnan Stone Forest, Yunnan Province, China. *Acta Ecologica Sinica*, (11): 1793-
599 1802+2020-2022, 2002.
- 600 Tian, Y., Zhang, J., Song, L., Bao, H.: A study on aerial algae communities on the surface of carbonate rock of
601 the Yunnan stone forest. *Carsologica Sinica*, (03): 39-47, 2003.
- 602 Tian, Y., Zhang, J., Song, L., Bao, H.: The role of aerial algae in the formation of the landscape of the Yunnan
603 Stone Forest, Yunnan Province, China. *Science in China, Series D: Earth Sciences*, 47(9): 846-864., 2004.
- 604 Timoncini, A., Costantini, F., Bernardi, E., Martini, C., Mugnai, F., Mancuso, F. P., et al.: Insight on bacteria



- 605 communities in outdoor bronze and marble artefacts in a changing environment. *Science of The Total*
606 *Environment*, 850: 1-14. <https://doi.org/10.1016/j.scitotenv.2022.157804>, 2022.
- 607 Wang, F., Han, H., Li, D., et al.: Study on the cleaning of black crusts on ancient marble carvings. *Sciences of*
608 *Conservation and Archaeology*, 36 (01): 65-73. [https://link.cnki.net/doi/10.16334/j.cnki.cn31-](https://link.cnki.net/doi/10.16334/j.cnki.cn31-1652/k.20231103084)
609 [1652/k.20231103084](https://link.cnki.net/doi/10.16334/j.cnki.cn31-1652/k.20231103084), 2024.
- 610 Wang, F.: study on the conservation of marble carvings in Beijing area. Doctoral Dissertation. Beijing: University
611 of Science and Technology Beijing. 1-181. <https://link.cnki.net/doi/10.26945/d.cnki.gbjku.2023.000238>,
612 2023.
- 613 Wang, J., Zhang, J., Zhang, X., et al.: Effects of nano super-hydrophobic protective coatings on the gas
614 permeability of rock materials. *Journal of Hebei University of Technology*, 49 (03): 63-68.
615 <https://link.cnki.net/doi/10.14081/j.cnki.hgdxb.2020.03.007>, 2020.
- 616 Wang, S.: The characteristic analysis of surface deterioration and mechanism study on West Yellow Temple
617 Stone heritage. Master's Thesis. Beijing: China University of Geosciences (Beijing). 1-57, 2010.
- 618 Warscheid, T., Becker, T. W., Resende, M. A.: Biodeterioration of stone: a comparison between (sub-)tropical
619 and moderate climate zones. *International Biodeterioration & Biodegradation*, 37(1): 124.
620 [https://doi.org/10.1016/0964-8305\(96\)84351-4](https://doi.org/10.1016/0964-8305(96)84351-4), 1996.
- 621 Warscheid, T., Braams, J.: Biodeterioration of stone: a review. *International Biodeterioration & Biodegradation*,
622 46(4): 343-368. [https://doi.org/10.1016/S0964-8305\(00\)00109-8](https://doi.org/10.1016/S0964-8305(00)00109-8), 2000.
- 623 Wu, M., Liu, J.: Fangshan Dashiwo and Stone Quarrying for Ming Dynasty Palaces and Tombs in Beijing - Also
624 on Stone Usage in Beijing's Imperial Construction Through Dynasties. *Proceedings of the Palace Museum*
625 (First Volume). 253-262, 1996.
- 626 Yang, X.: Study on Weathering mechanism of Beijing Marble. Master's Thesis. Beijing: China University of
627 Geosciences (Beijing): 1-92, 2016.
- 628 Ye, J., Zhang, Z.: Correlation Study of Physical and Mechanical Parameters of Beijing Marble. *Journal of*
629 *Engineering Geology*, 27 (3): 532-538. <https://link.cnki.net/doi/10.13544/j.cnki.jeg.2018-102>, 2019.
- 630 Zhang, G.: Research on the weathering mechanism and Protection technology of spalling disease of Marble
631 relics in Beijing. Master's Thesis. Beijing: Beijing University of Chemical Technology. 1-77.
632 <https://link.cnki.net/doi/10.26939/d.cnki.gbhgu.2022.000801>, 2022.
- 633 Zhang, G., Gong, C., Gu, J., Katayama, Y., Someya, T., Gu, J.: Biochemical reactions and mechanisms involved



- 634 in the biodeterioration of stone world cultural heritage under the tropical climate conditions. *International*
635 *Biodeterioration & Biodegradation*, 143: 1-8. <https://doi.org/10.1016/j.ibiod.2019.104723>, 2019.
- 636 Zhang, T., Li, D., Zhang, Z.: Damage categories and deterioration mechanism of stone cultural relics of white
637 marble in Beijing. *Geotechnical Investigation & Surveying*, 44 (11): 7-13, 2016.
- 638 Zhang, Z., Yang, X., Ye, F., et al.: Microscopic characteristics of petrography and discussion on weathering
639 mechanism of Fangshan marble in Beijing. *Journal of Engineering Geology*, 23 (02): 279-286.
640 <https://link.cnki.net/doi/10.13544/j.cnki.jeg.2015.02.013>, 2015.
- 641 Zhang, Z., Zhao, Y., Su, Z.: Survey and evaluation of building materials of the Yan Qing Tang site in the Yuan
642 Ming Yuan ruin. *Sciences of Conservation and Archaeology*, 25 (04): 96-99.
643 <https://link.cnki.net/doi/10.16334/j.cnki.cn31-1652/k.2013.04.008>, 2013.
- 644 Zhao, B.: The research on protection of marble relics by environmentally friendly surface preservative coatings.
645 Master's Thesis. Beijing: Beijing University of Chemical Technology. 1-103, 2018.
- 646 Zhu, H.: *Freshwater Algae in China (Volume 2, Orders Chroococcales)*. Beijing: Science Press. 1-105, 1991.